http://dx.doi.org/10.5012/bkcs.2011.32.11.3861

Surface Plasmon Enhanced Photoluminescence of Rhodamine B Confined in SBA15

K. Dinakaran,[*] A. Chandramohan,[†] M. R. Venkatesan,[†] S. Devaraj,[†] V. Devi, and M. Alagar[†]

Department of Chemistry, MIT Campus, Anna University, Chennai – 600044, India. [*]E-mail: kdinakaran.auc@gmail.com
[†]Department of Chemical Engineering, A.C. Tech Campus, Anna University, Chennai – 600025, India
Received May 20, 2011, Accepted August 31, 2011

Rhodamine B dye (RB) has been introduced into the mesoporous silica (SBA15) and Ag anchored mesoporous silica by applying solution impregnation method. Surface treatment of SBA15 with 3-aminopropyltrimethoxysilane (APTMS) facilitates selective anchoring of the RB molecules on SBA15. The photoluminescence spectra of RB confined within SBA15 indicates higher emission intensity, than that of the RB solid, particularly in the presence of Ag nanoparticles. The significant enhancement in photoluminescence intensity is attributed to the local enhancement of the optical fields near the molecules by interactions with silver plasmons.

Key Words : SBA15, Rhodamine-B, Photoluminescence, SPR, Sol-gel

Introduction

Fluorescent Organic dyes, encapsulated in various hosts, represent attractive materials for optical data storage, frequency doubling, microlasing, optical sensing, or photocatalysis because of their large fluorescent bandwidths covering entire visible spectrum.[1-3] Usually it is the type of host, for dyes, that determines the characteristics of the fluorescence signals and its end user applications. For example, organic dye molecules have been doped into various host materials such as polymers,[4,5] sol-gel glass,[6] mesoporous silica (MCM-41),[7] thin films[8,9] and fibres.[10] Out of these host materials, mesoporous silica materials provide a confined space for the controlled intrapore inclusion for organic dye molecules because of their high surface areas, narrow pore size distribution and well-defined pore networks.[11]

The organic fluorescent dye molecules entrapped mesoporous nanostructure has been widely studied for its use as fluorescent probes for bioanalysis because of the photostability offered by chromophores confined within the mesoporous channels and the silica surface serves as a versatile substrate for the immobilization of biomolecules. Especially, ordered mesoporous silica with large pore diameters and uniform nanoparticle sizes can be utilized for the controlled release of drugs and DNA.[12] Thus, the dye-doped mesoporous silica nanoparticles (dye-MSNs) can play a multifunctional role as a biomarker, bioimaging indicator and drug carrier for disease diagnosis and synchronous therapy.

The most important requirement for an efficient fluorescent biosensor, based on the organic dye confined in an inorganic host, is the high quantum efficiency of light emission. Few attempts have been made to improve efficiency of dye confined in mesoporous channels by varying the synthetic methodology. For example, Tan and co-workers have synthesized dye-doped silica nanoparticles by a reverse microemulsion method.[13] However, the fluorescence emission wavelength has a large red shift owing to the physical adsorption and aggregation among dye molecules and their fluorescence quantum yield is also relatively lower due to the concentration quenching effect, which subsequently lowers fluorescence detectivity. Shi *et al.* immobilized Rhodamine B dyes on SBA15 by covalent bonding to avoid self quenching to a large extent which enhances the fluorescence intensity, quantum yield and photostability, and thus the fluorescence detectivity enhanced. However, its light-emission efficiencies are still substantially lower due to the limited number of molecules anchored on SBA15.[14]

One of the most advanced techniques available to enhance efficiency of dye emission is surface plasmon coupling.[15] Photoluminescence of molecules near noble metal surfaces is enhanced by both absorption enhancement and the emission enhancement.[16] Silver is the most commonly used metal since its plasmon resonances are typically in the visible region with high quality factor. In this research, we report the inclusion and photoluminescent properties of Rhodamine B base (RB) dye molecules and silver nanoparticle into the mesoporous siliceous framework (SBA15) through post synthetic incorporation method.

Experimental

Materials. Pluronic P123 (ethylene oxide (EO)-propylene oxide (PO) triblock copolymer, composition as $EO_{20}PO_{70}EO_{20}$, was purchased from Polymer Source, Inc. The number average molecular weight of P123 is about 5300. Tetraethylorthosilicate (TEOS), Rhodamine B base and silver nitrate were purchased from Aldrich. Analytical grade hydrochloric acid was purchased from Laborbedarf GmbH. Milli Q water was used in all experiments.

Materials Preparation. SBA15 was prepared according to literature[16] from batches of 2 g Pluronic P123 (ethylene oxide (EO)-propylene oxide (PO) triblock copolymer, 15 g H_2O, 60 g 2M HCl, 4.25 g TEOS. The mixture was kept under stirring at 313 K for 24 h and then heated at 373 K temperature for another 24 h under static conditions for aging. The white precipitate was filtered, washed with water,

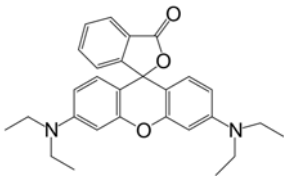

Scheme 1. Chemical structure of Rhodamine B base.

air-dried at room temperature. The resulting powder was calcined in 773 K at the rate of 2 K min in air. Then a proper amount of SBA15 was dispersed into an ethanol solution of APTMS and refluxed for about 24 h at 80-90 ºC. The product (H_2N-SBA15) was recovered by filtration and washed with ethanol and dried in air. Silver loading about 8% was achieved by adding 2 mL of 1% aqueous solution of $AgNO_3$ to 50 mg of H_2N-SBA15. The mixture was continuously stirred for 30 min. Reduction of Ag (0) was performed by adding 1 mL of a 0.1 M $NaBH_4$ aqueous solution to 50 mg of the $AgNO_3$ adsorbed H_2N-SBA15 and stirred for 30 min. The product was recovered by centrifugation, washed with distilled water and air dried. The mesoporous silica and Ag adsorbed mesoporous silica were soaked in 0.01 M aqueous solution of Rhodamine B base for 15 min and the content was filtered and air dried. The amount of adsorbed dye was calculated by thermo gravimetric analysis.

Characterization. High-resolution transmission electron microscopy (HRTEM) and energy dispersive spectroscopy (EDS) measurements were carried out on a JEOL JSM2100-F at 100 kV. UV-vis absorption studies were carried out using a UV-vis-Near IR spectrophotometer (Varian, Cary 5000). Photoluminescence was recorded in Perkin Elmer fluorescence spectrometer. FTIR spectra were recorded in a Perkin Elmer spectrometer.

Results and Discussion

The SBA15 host material was synthesized using P123, a triblock copolymer of EO-PPO-EO, as template. After removing the template by calcinations, the APTMS molecules were introduced into the channels of SBA15 by post synthetic functionalization method, which leads to the amino functionalization at the internal walls of SBA15 channels. The $AgNO_3$ precursor and reducing agents were then introduced into aqueous dispersion of SBA15. The Ag(0) nanoparticles were formed through the reduction of Ag(I) ions by reducers and these Ag nanoparticles were attached to the amino functional groups at the walls of the SBA15, since amine has specific affinity towards metal surfaces. The silver nanoparticles assembled inside the channels of SBA15, were further confirmed by HRTEM and N_2 sorption studies.

Figure 1(a) shows the HRTEM of calcinated SBA15, in which a well ordered channels are illustrated and are characteristic of mesoporous materials. Figure 1(b) depicts the HRTEM of Ag-SBA15, where the highly ordered pore structure of SBA15 is still preserved. We can observe clearly that silver nanoparticles appear as dark spherical objects

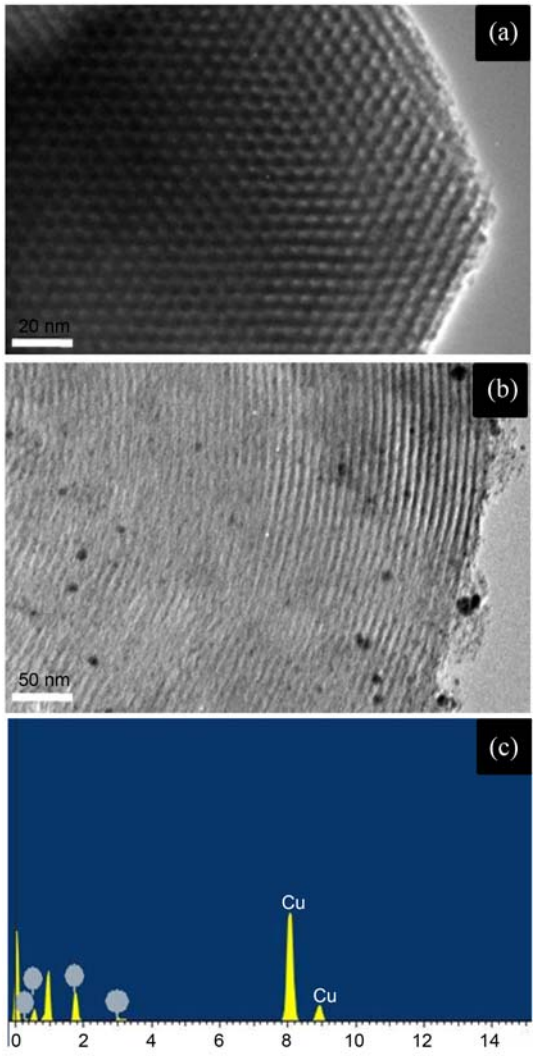

Figure 1. The HRTEM of (a) calcinated SBA15, (b) Ag-SBA15 and (c) EDS spectra of Ag-SBA15.

between the walls of SBA15 and are distributed inside the channels of SBA15 as well as at the surface of the particle. The chemical identity of the hybrid film was also confirmed by EDS data, where the presence of Ag and SiO_2 is evident in Figure 1(c).

Figure 2 shows that the inclusion of Ag nanoparticle on the surface of SBA15 brought about a decrease in the nitrogen adsorption capacity, which reflects a decrease in the specific surface area of the sample. However, the position and the height of hysteresis, which are in proportion to the mesopore diameter and the mesopore volume, respectively, decrease slightly after the inclusion of the nanoparticle. The pore volumes of Ag-SBA15 decreases as the concentration of Ag loading increased. For example, the SBA15 is impregnated separately in 0.004 M and 0.2 M solution of $AgNO_3$, after reducing to Ag, the corresponding average pore volumes of the samples are 1.306 $cm^3\ g^{-1}$ and 0.9454 $cm^3 g^{-1}$, thus the amount of loaded metal Ag may be located on the pores of the support.

Diffuse reflectance UV-vis spectra of the Ag impregnated

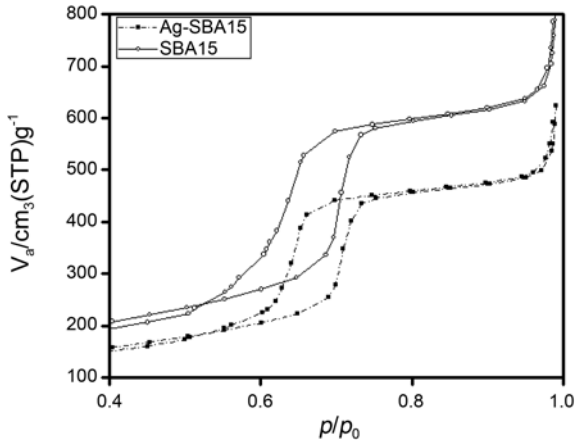

Figure 2. Nitrogen adsorption-desorption isotherms of SBA15 and Ag-SBA15.

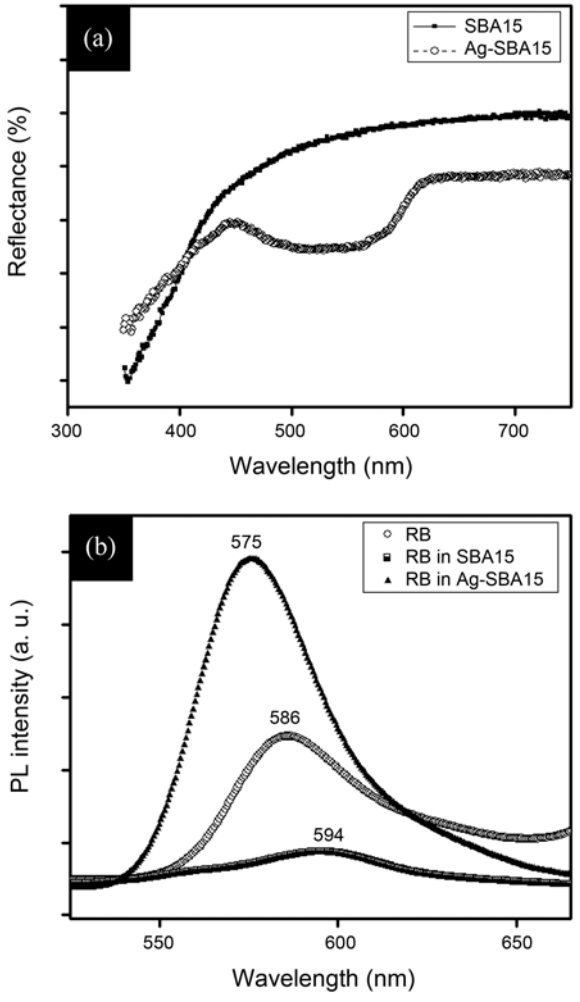

Figure 3. (a) Diffuse reflectance UV-visible spectra of SBA15 and Ag-SBA15. (b) Photoluminescence spectra of RB, RB confined in SBA15 and RB confined in Ag-SBA15.

SBA15 was recorded using a Perkin Elmer spectrophotometer lambda 900, equipped with an integrating sphere. The spectrum is as shown in Figure 3(a). The absorption maxima of Ag nanoparticles anchored on SBA15 is observed between 450 and 621 nm which corresponds to the visible range of the spectrum. This characteristic peak is due to the oscillation of conduction band electrons of Ag, known as the surface plasmon resonance.[18] The broad nature of the absorption band in this case is indicative that Ag is located within silica channels.

Figure 3(b) Rhodamine B base exhibits an intense emission spectrum at 586 nm in the solid state. When it has been immobilized on SBA15, the emission maximum is observed at 594 nm. This shows that the fluorescence spectrum of Rhodamine B has significantly red shifted to about 8 nm, indicating that the electronic environment around RB is different, since the fluorescence wavelength is subject to the microenvironment around the molecule. This result is further explained as the reduction of the HOMO-LUMO band gap by the confinement of dye within mesoporous silica, resulting in the red shift of absorption spectra.[19,20] The intensity of maximum emission of RB in SBA15 significantly decreased compared with solid RB. The decrease emission intensity of RB may be explained by the electronic interaction between the dye molecules and surface of SBA15, which results in the energy transfer from excited state of RB to SBA15 and low fluorescence emission intensity. A significant blue-shift of the fluorescence spectrum of Rhodamine B base was observed with silver nanoparticle overlayers. Our interpretation is that the spectral shifts can be associated with the plasmon resonance of Ag nanoparticle. The effects of scattering or reabsorption of the emitted light by the silver may tend to blue-shift the spectrum. Besides, the interaction of dye with the nanoparticle transition dipoles that shifts the emission maximum towards the plasmon resonance of Ag nano particle. Further, the intensity of the emission spectrum of Ag-SBA15-RB has greatly enhanced compared to the intensity of SBA15-RB in the wavelength of 575 nm. This is consistent with borrowing the oscillator strength from the silver plasmon resonance through a dipolar coupling mechanism. This shows a significant achievement in enhancing the emission intensity of dye confined in mesoporous channels. Significant PL increases are obtained throughout the spectrum since there is a large distribution of surface plasmon resonance frequencies due to interactions between the silver nanoparticles.[15]

Conclusion

To summarize, a simple and efficient way of enhancing the photoluminescence of Rhodamine B base confined within mesoporous channels has been demonstrated. Deposition of silver nanoparticles directly onto mesoporous silica resulted in dramatic enhancement of photoluminescence of Rhodamine B. This synthetic strategy and luminescence efficiency of mesoporous nanomaterials can be useful to develop fluorescence sensors for medical diagnostic applications.

References

1. Yang, P.; Wirnsberger, G.; Huang, H. C.; Cordero, S. R.; Scott, B.;

McGehee, M. D.; Deng, T.; Whitesides, G. M.; Chmelka, G. F.; Buratto, S. K.; Stucky, G. D. *Science* **2000**, *287*, 465.
2. Ganschow, M.; Wark, M.; Weohrle, D.; Schulz-Ekloff *Angew. Chem. Int. Ed*. **2000**, *39*, 161.
3. Wirnsberger, G.; Stucky, G. D. *Chem. Phys. Chem*. **2000**, *1*, 89.
4. O'Connel, R.; Saito, T. *Opt. Eng.* **1983**, *22*, 393.
5. Sastre, R.; Costela, A. *Adv. Mater.* **1995**, *7*, 198.
6. Narang, U.; Wang, R.; Prasad, P.; Bright, F. *J. Phys. Chem.* **1994**, *98*, 17.
7. (a) Beck, J. S. *J. Am. Chem. Soc*. **1992**, *114*, 10834. (b) Shao, Y.; Wang, L.; Zhang, J.; Anpo, M. *J. Photochem. Photobiol. A* **2006**, *180*, 59.
8. Schacht, S.; Hou, Q.; Voift-Martin, I. G.; Stucky, G. D.; Schuth, F. *Science* **1996**, *273*, 768.
9. Yang, H.; Kuperman, A.; Coombs, N.; Mamicheafara, M.; Ozin, G. A. *Nature* **1996**, *379*, 703.
10. Huo, Q.; Zhao, D.; Feng, J.; Weston, K.; Buratto, S. K.; Stucky, G. D.; Schacht, S.; Schuth, F. *Adv. Mater*. **1997**, *9*, 974.
11. Kresge, C. T.; Leonowicz, M. E.; Roth, W. J.; Beck, J. S. *Nature* **1992**, *359*, 710.
12. (a) Zhu, Y. F.; Shi, J. L.; Shen, W. H.; Dong, X. P.; Feng, J. W.; Ruan, M. L.; Li, Y. S. *Angew. Chem. Int. Ed*. **2005**, *44*, 5083. (b) Jin, H. Y.; Qiu, H. B.; Sakamoto, Y.; Shu, P.; Terasaki, O.; Che, S. A. *Chem.-Eur. J.* **2008**, *14*, 6413. (c) Radu, D. R.; Lai, C. Y.; Jeftinija, K.; Rowe, E. W.; Jeftinija, S.; Lin, V. S.-Y. *J. Am. Chem. Soc*. **2004**, *126*, 13216. (d) Zhang, H. J.; Wu, J.; Zhou, L. P.; Zhang, D. Y.; Qi, L. M. *Langmuir* **2007**, *23*, 1107. (e) Slowing, I. I.; Trewyn, B. G.; Giri, S.; Lin, V. S.-Y. *Adv. Funct. Mater*. **2007**, *17*, 1225.
13. (a) Santra, S.; Zhang, P.; Wang, K.; Tapec, R.; Tan, W. *Anal. Chem*. **2001**, *73*, 4988. (b) Shibata, S.; Taniguchi, T.; Yano, T.; Yamane, M. *J. Sol-Gel Sci. Technol*. **1997**, *10*, 263.
14. He, Q.; Shi, J.; Cui, X.; Zhao, J.; Chen, Y.; Zhou, J. *J. Mater. Chem.* **2009**, *19*, 3395.
15. (a) Neal, T. D.; Okamoto, K.; Scherer, A. *Optic Exp.* **2005**, *13*, 5522. (b) Kalele, S.; Deshpande, A. C.; Singh, S. B.; Kulkarni, S. K. *Bull. Mater. Sci*. **2008**, *31*, 541. (c) Jiang, Y.; Wang, H. Y.; Wang, H.; Gao, B. R.; Hao, Y. W.; Jin, Y.; Chen, Q. D.; Sun, H. B. *J. Phys. Chem. C* **2011**, *115*, 12636. (d) Mitamura, K.; Imae, T.; Tian, S.; Knoll, W. *Langmuir* **2008**, *24*, 2266.
16. Shanlin, P.; Wang, Z.; Lewis, J. R. *J. Phys. Chem. B* **2006**, *110*, 17383.
17. Jiang, Q.; Wu, Z. Y.; Wang, Y. M.; Cao, Y.; Zhou, C. F.; Zhu, J. H. *J. Mater. Chem.* **2006**, *16*, 1536.
18. (a) Itakura, T.; Torigoe, K.; Esumi, K. *Langmuir* **1995**, *11*, 4129. (b) Foss, C. A.; Hornyak, G. L.; Stockert, J. A.; Martin, C. R. *J. Phys. Chem*. **1994**, *98*, 2963. (c) Link, S.; Mohamed, M. B.; El-Sayed, M. A. *J. Phys. Chem. B* **1999**, *103*, 3073. (d) Jana, N. R.; Gearheart, L.; Murphy, C. J. *J. Phys. Chem. B* **2001**, *105*, 4065. (e) Cepak, V. M.; Martin, C. R. *J. Phys. Chem. B* **1998**, *102*, 9985.
19. Marquez, F.; Garcy, H.; Palomares, E.; Fernandez, L.; Corma, A. *J. Am. Chem. Soc*. **2000**, *122*, 6520.
20. Zhang, L. Z.; Cheng, P.; Tang, G. Q.; Liao, D. Z. *J. Lumin*. **2003**, *104*, 123.